Nonequilibrium emission of neutrons from fusion-like reactions of 152-MeV ^{16}O with ^{154}Sm

K. Geoffroy Young* and D. G. Sarantites
Department of Chemistry, Washington University, St. Louis, Missouri 63130

J. R. Beene, M. L. Halbert, D. C. Hensley, and R. A. Dayras†
Oak Ridge National Laboratory, Oak Ridge, Tennessee 37830

J. H. Barker‡
Department of Physics, St. Louis University, St. Louis, Missouri 63103

(Received 1 December 1980)

Neutron time-of-flight spectra and angular correlations were obtained in coincidence with γ rays characteristic of the xn (x = 8,9,10) and αxn (x = 7,8) fusion-like products in reactions of 151.9 MeV ^{16}O with ^{154}Sm. The spectra at all angles (20°, 70°, 100°, 151°) clearly indicate the presence of nonequilibrium neutron emission. The energy spectra can be represented in terms of isotropic emission in the rest frames of two moving sources. The slower of these moves with the speed of the center of mass; its emission corresponds to a temperature of ~1.7 MeV. The faster source, characterized by a temperature of 5 to 6 MeV, has a velocity of ~0.4 of that corresponding to the projectile energy above the Coulomb barrier. The yield of fast neutrons as a function of the exit channel is found to be in good agreement with the predictions of an extended incomplete fusion model. Comparisons are made with other models that lead to emission of fast neutrons.

[NUCLEAR REACTIONS $^{154}Sm(^{16}O, xn)^{170-x}Yb$ x=8–10; $^{154}Sm(^{16}O, \alpha xn)$ $^{166-x}Er$, x=7,8; E=151.9 MeV; measured $\sigma(E_n, \theta_n)$; deduced temperatures, source velocities and yields of equilibrium and pre-equilibrium neutrons, interaction times; compared with incomplete fusion, PEP, and hot-spot models.]

I. INTRODUCTION

Nonequilibrium emission of particles is well known in fusion reactions induced by light ions,[1] but for heavy-ion reactions, investigations of this effect are sparse. A characteristic feature of nonequilibrium emission of particles is the presence of a high-energy, forward peaked component in the energy spectra of the emitted particles. This was first observed by Britt and Quinton[2] in singles spectra of charged particles from reactions of ^{12}C, ^{14}N, and ^{16}O on Au and Bi targets at 10.5 MeV/nucleon of incident laboratory energy and later by Galin *et al.*[3] in reactions of ^{14}N on ^{103}Rh at 5.8 and 8.6 MeV/nucleon. Since in addition to fusion other processes such as deeply inelastic and quasielastic reactions are now known to occur under the above conditions, detection techniques must be used which associate the nonequilibrium emission with the appropriate process. During the past few years, experiments specifically designed to select particles associated with the fusionlike exit channels have been carried out, usually by selecting particles in coincidence with γ rays characteristic of the de-excitation of individual residual nuclei.[4-13] Evidence from γ-ray side feeding patterns,[6,8,11,13] excitation functions,[10] and γ-ray multiplicities[12] indicates that the high-energy forward-peaked charged particles originate from a narrow range of partial waves at high l in the entrance channel.

Such reactions have been called incomplete fusion,[6,10] massive transfer,[8,14] or breakup fusion.[15] Several models have been proposed to describe them: the classical generalized critical angular momentum model[10] and two quantum-mechanical models involving distorted-wave calculations.[14,15] All assume that the fast particles are essentially spectators and have left the scene before fusion is complete. They predict that the interaction is predominantly peripheral (large impact parameters). Other models of nonequilibrium emission have been proposed for heavy-ion reactions in this energy range. In one class of models (precompound emission,[1] hot spots[16]) the fast particles are emitted from localized regions of high excitation before energy equilibration is complete. In another class [Fermi jets,[17] prompt emission of particles (PEP)[18,19]] the high particle-emission energies arise from the coupling of the internal Fermi motion with the relative motion of the colliding nuclei. Both of these classes of models may involve central collisions (small impact parameters).

The angular distribution of the energetic charged particles is affected by the Coulomb field which may cause focusing[17] or shadowing[20] effects. Therefore it seems worthwhile to investigate

neutron emission in spite of the additional experimental complexity associated with neutron measurements. Another reason for studying neutrons is that the role of the Fermi motion should be more clearly visible in the emission of nucleons than of larger fragments.

Neutron spectra associated with various heavy-ion fusion channels have been measured by means of the γ-ray coincidence technique.[7] For ^{158}Gd bombarded with ^{12}C at 12.7 MeV/nucleon (compound nucleus $^{170}_{70}$Yb), Westerberg *et al.*[7] found a substantial nonequilibrium component in the neutron spectra associated with various isotopes of $_{70}$Yb and $_{68}$Er. In contrast, no nonequilibrium neutrons appear for 8.7 MeV/nucleon ^{20}Ne on ^{150}Nd even though this system leads to the same compound nucleus at the same excitation energy.[7] In a recent experiment in which fusion events were selected by detection of evaporation residues, Petitt *et al.*[21] have found a nonequilibrium component in the spectra of neutrons from reactions of 208-MeV ^{16}O and ^{93}Nb. The same experiment also revealed that an excess of high-energy neutrons is in coincidence with deep-inelastic fragments. A similar result has been reported[22] for ^{16}O + ^{58,64}Ni; earlier searches for such effects in strongly damped collisions were negative.[23,24] An attempt to systematize such observations was made by Hilscher *et al.*[23] They tried to correlate the projectile energy per nucleon above the Coulomb barrier with the presence or absence of nonequilibrium effects, but the paucity of data did not permit firm conclusions.

We have discussed in other papers[7,25,26] the relationship between saturation of the γ-ray multiplicity $\langle M_\gamma \rangle$ as a function of bombardment energy in particular (HI, xn) exit channels and the occurence of nonstatistical neutron emission. It is shown in Ref. 26 that the variation with projectile energy of $\langle M_\gamma \rangle$ in particular xn channels can be accounted for quantitatively by assuming a mechanism of incomplete fusion[10] that is localized in angular momentum near l_c, the maximum angular momentum participating in complete fusion. The incomplete fusion picture of Siwek-Wilczynska *et al.*[10] does not make definite predictions about the shape of the neutron spectrum, but the spectra would be expected to exhibit the characteristics of emission from a source (the projectile) moving rapidly in the center of mass system. The model does lead to definite predictions about the relative yield of fast and equilibrium neutrons from individual xn channels.[26] Comparisons of results from the neutron spectra with these predictions will serve to test the validity of this picture.

Predictions of neutron energy spectra, angular distributions and cross sections for the non-equilibrium neutron emission have been made by the PEP model of Bondorf *et al.*[18,19] which is based on the coupling of the internal Fermi motion with the relative velocity of the colliding nuclei. Central collisions are believed[19] to play a larger role in this model than that of Ref. 10. This may lead to different shapes of the fast neutron spectrum and/or of the angular distributions.

In view of the marked difference[7] between ^{12}C + ^{158}Gd and ^{20}Ne + ^{150}Nd, it seemed desirable to study neutron emission from the ^{170}Yb composite system with a projectile intermediate between ^{12}C and ^{20}Ne. The system chosen was ^{16}O on ^{154}Sm at a bombarding energy of 151.9 MeV since other experiments[9,26] had shown that secondary effects of nonequilibrium emission are evident in this system, namely long-tailed excitation functions and saturation of the average γ-ray multiplicity with increasing bombarding energy.

The neutron spectra were obtained by the time-of-flight method in four detectors at angles from 20° to 151°. The angular distributions are more complete than in our earlier work[7] and provide more information for the understanding of the reaction mechanism.

II. EXPERIMENTAL METHODS

The apparatus and methods of analysis were basically similar to those used in the study of ^{12}C + ^{158}Gd by Westerberg *et al.*[7] except that the reaction chamber was the larger one (49.5-cm diam) described in Ref. 27. The experimental arrangement included six light-particle telescopes in the median plane (horizontal) and the "Urchin" array of seven individually shielded NaI detectors[27] mounted below the chamber. Data were obtained simultaneously from the telescopes and the neutron detectors. Only the neutron spectra and angular distributions will be presented here; a brief account of the charged-particle spectra and the associated γ-ray multiplicity data has been published.[12] The counting statistics for the high-energy neutrons were not adequate for determination of the associated γ-ray multiplicity.

A. Beam and target

A 152.9-MeV $^{16}O^{5+}$ beam from the Oak Ridge Isochronous Cyclotron bombarded a 1.3 mg/cm^2 rolled target of samarium metal enriched to 98.69% in ^{154}Sm. The target was tilted at 10° to the beam direction and mounted on a frame bent at 20° to avoid shadowing of any detector. The

effective target thickness was 1.4 mg/cm^2. The mean energy of bombardment was 151.9 MeV, corresponding to an excitation of 121.0 MeV in the compound nucleus ^{170}Yb.

As in all earlier experiments of this series,[7,25,28,29] the beam was focused on the target nondispersively by means of a crossover in the switching magnet.[30] The only beam collimator was at this crossover; none were used in the vicinity of the reaction chamber. The target spot was ≤ 2 mm in diameter, much smaller than the aperture in the target frame (17.5-mm diam), and there was no indication of a halo. The beam passed through the target and was collected in a large Faraday cup (10-cm diam, 1.7-m long).

B. Detectors

The Ge(Li) detector was placed 7.6 cm from the target at 45° on the side of the beam opposite to the particle telescopes. The counting rate in this detector was kept below 8000 counts/s by limiting the beam intensity to 3 nA. The photopeak efficiency as a function of γ-ray energy was deduced from measurement with γ-ray sources of known strength placed at the target position.

The neutrons were detected in four large plastic scintillators (NE-102), 7.6-cm-thick cylinders of diameter 30.5 cm with their axes intersecting the beam spot on the target. Each one was viewed through air at a distance of 30 cm by a 13-cm diam 2.0 ns-risetime phototube (RCA-4522). A conical housing coated on the inside with TiO_2 reflective material supported each scintillator-phototube combination. Two of these detectors had been used in the $^{12}C + ^{158}Gd$ measurements.[7] The detector axes were in the median plane at polar angles $\theta = 20°$, 70°, 100°, and 151° on the same side of the beam as the Ge(Li) detector. The entrance faces were at distances of 110, 100, 90, and 80 cm, respectively, from the target. Their efficiencies for neutron detection as a function of pulse-height threshold were taken from Monte Carlo calculations for various neutron energies described in Sec. II B of Ref. 7. Setting of the thresholds and a check of the efficiency are described in the next section.

Events with time of flight longer than that corresponding to 2-MeV neutrons were discarded because of (a) possible contamination with scattered neutrons (the test described in Ref. 7 showed such contamination should be negligible above 2 MeV), and (b) uncertain neutron efficiency at such energies (the minimum threshold used corresponds to the maximum light output obtained from 1.5 MeV neutrons).

Neutron interactions with the material near the target can introduce systematic errors in the absolute cross sections and spectrum shapes. The ports of the reaction chamber were covered with 0.6 cm Al plates and the wall between the ports reached a maximum thickness of 1.2 cm Al. The outscattering of neutrons initially headed for the detectors is estimated to be only a few percent and no correction was applied to the absolute cross sections. Scattering of neutrons in the chamber walls should not affect the spectrum shape significantly since the total cross section in the energy range of interest varies little with neutron energy and is dominated by elastic scattering. Inscattering from the massive Pb shield of the Urchin, as mentioned above, was shown to be negligible above 2 MeV by the shadow-shield test of Ref. 7; the shadow shield was carefully shaped and positioned to minimize attenuation of the background radiation produced by the Urchin.

Energetic neutrons may be simulated by delayed γ rays from isomers produced in the target and from $(n,n'\gamma)$ events in the Urchin shield or the chamber walls, but the following arguments indicate that these effects were not significant. First, most of the reactions lead to nuclei that are good rotors and we therefore do not expect significant yields of isomeric states with few-ns lifetimes. Second, both types of background should be correlated only weakly with detector angle, but as will be seen later the energetic component of the neutron spectrum changes significantly with both angle and channel. Finally, we reiterate that in the $^{20}Ne + ^{150}Nd$ reaction, which was studied with very similar apparatus, events corresponding to high energy neutrons are practically absent.[7]

C. Data acquisition and analysis

A coincidence between the Ge(Li) detector and any of the scintillator triggered circuits that digitized the linear signals and then transmitted the results to the on-line computer (SEL-840A). The data for each such event included the Ge(Li) pulse height, a timing signal, the scintillator pulse height, and a bit pattern telling which counter(s) had fired. The data-acquisition program wrote the data on tape, event by event. It also offered, for purposes of monitoring, several options for on-line display of the data during accumulation.

The timing signal was generated by a time-to-amplitude converter (TAC). The start pulse was obtained from a coincidence between the Ge(Li) logic signal and one of the train of pulses derived from the cyclotron rf (repetition period 111.2 ns). The stop pulse came from the plastic scintillator. Full scale on the TAC corresponded to over 3 rf periods. The time spectra typically showed a

sharp peak ("γ flash") at short times due to γ rays detected in the scintillator and, at longer times, a broad continuum due to neutrons with approximately equal total intensity. Two small peaks were observed due to random coincidences of a Ge(Li) pulse with the γ flashes of the next two beam bursts. These gave an accurate calibration of the time scale and a measure of the random coincidences ($<0.5\%$).

For data accumulated over periods of several minutes, the time resolution of the prompt flash was typically 3 ns full width at half maximum (FWHM), increasing to ~4 ns for the lowest pulse heights of interest. However, cyclotron tuning and slow drifts often changed the phase of the beam bursts with respect to the rf by several ns, as had been noted earlier.[7] These shifts were largely eliminated during the tape playback. The scanning program calculated the centroid of the γ flash for each group of 500 prompt events and evaluated the timing of the next group of events with respect to this centroid. The choice of 500 prompt coincident events in each neutron detector, based on the need for adequate statistics for locating the centroid, corresponded to adjustments of the centroid roughly 10 times/min during the cyclotron run; this was adequate to eliminate the slow drifts entirely. The energy resolution for the detector at 110 cm was ± 0.15 MeV for 2.5-MeV neutrons and $+1.4$, -1.2 MeV for 10.5-MeV neutrons. For the closest (80 cm) detector, the corresponding figures are ± 0.2 MeV and $+2.0$, -1.6 MeV.

The scintillator pulse-height information was used during playback to discriminate against γ rays detected by the scintillators. First, some tape was scanned to generate a two-parameter plot of pulse height vs time of flight for each scintillator. Nearly all of the unwanted γ-ray events in this array were found to be well separated from the neutron events. When the tapes were played back to produce the Ge(Li) spectra (Sec. II D), software masks accepting only neutron events in each scintillator were incorporated in the program. The locus of the prompt γ-ray events in the two-parameter arrays also provided a measurement of the amplitude dependence of the timing ("walk"). Although the effect was minor, certainly much smaller than in the previous work[7] due to use of better discriminators, it was corrected during playback of the tapes.

The neutron-counter efficiencies were taken from Monte Carlo calculations described in Sec. II B of Ref. 7. The effective thresholds were determined by the lower boundaries of the masks and were different for each time bin. For the longest times the lower boundary corresponded to the maximum pulse height deposited by 1.5-MeV neutrons; for the short times (high energy neutrons) it corresponded to 2.2 MeV. A trial scan with another mask starting at a higher pulse height gave a decrease in the number of neutron events exactly as predicted by the efficiency calculations, thus giving confidence in their accuracy.

As mentioned earlier, the experiment included six charged-particle telescopes. The number of linear signals that could occur in one event was thus very large (21), far more than the number of available digitizing circuits. Groups of signals were therefore multiplexed, with the contributions from the individual detectors sorted out on playback by means of the identification bits. The pulse-height signals from the four scintillators shared one amplifier and all the timing signals went to one TAC. Events in which more than one neutron detector fired could therefore not be used and were discarded during tape playback. From the geometry, efficiencies, and average neutron multiplicity (~9 from the data of Ref. 26) one expects about 4% of the neutron events to include detection of a second neutron. However, since the number of events in the γ flash was about equal to the number of neutrons, the fraction of multiple events should have been 8%; this includes events in which an otherwise valid neutron event was lost because a prompt γ was detected in the same scintillator. This expectation was borne out by examining a small sample of scintillation-counter events from one tape: out of 334 events, 27 (8.1%) were found to be accompanied by a pulse in one of the other scintillators. The yields were accordingly increased by 8% when the cross sections were calculated.

D. Ge(Li) spectra and cross sections

The data finally produced from the tape playback consisted of four series of Ge(Li) spectra, one series for each scintillator, for time windows corresponding to various intervals of neutron energy. Peak areas were then extracted for two or three low-lying characteristic transitions in ^{162}Yb, ^{161}Yb, and ^{160}Yb ($8n$, $9n$, and $10n$ channels) and in ^{159}Er and ^{158}Er ($\alpha 7n$ and $\alpha 8n$ channels) by use of a semiautomatic peak-fitting program. Fits were first made to groups of one to five peaks in a spectrum with good statistics [usually the sum of all Ge(Li) spectra over all time bins and angles]. The peak position and width parameters were then held fixed for fits of the same peaks in the individual spectra.

The peak areas were converted to double-differential neutron cross sections per unit solid angle and unit energy with the known counter solid

angles and efficiencies, target thickness, and integrated beam current. The ^{16}O ions were assumed to be fully stripped after passing through the target. Corrections were included for internal conversion, target tilt, and the multiple-event loss referred to in the preceding section. The n-γ angular correlation effects were not calculated; they should be small because the Ge(Li) detector was placed at 45°, near the zero of $P_2(\cos\theta)$.

At each angle the neutron spectra for the two or three transitions belonging to the same product nucleus were of similar shape. For improved statistics, they were combined in a weighted average and normalized to the intensity in coincidence with one transition in each nucleus (the $2^+ \rightarrow 0^+$ transition for ^{162}Yb and ^{158}Er, the $4^+ \rightarrow 2^+$ for ^{160}Yb, and the $\frac{17}{2}^+ \rightarrow \frac{13}{2}^+$ for ^{161}Yb and ^{159}Er) since these transitions had, within the uncertainties, the same relative intensities as the total cross sections measured earlier[26] with much better statistics. With the exception of ^{161}Yb, there is no branching above these transitions. The side feeding of levels below these transitions was assumed to be insignificant. Thus the cross sections observed for these γ rays were taken as the cross sections for the corresponding channels. The situation is more complicated for ^{161}Yb, where in similar reactions new data[31] have shown that parallel bands are appreciably populated and about half the de-excitations do not go through the $\frac{17}{2}^+ \rightarrow \frac{13}{2}^+$ (232-keV) transition. Accordingly, the cross section for the $9n$ channel was obtained by doubling the observed cross section for the 232-keV transition. A similar procedure was found necessary in studies of $^{12}C + ^{158}Gd$ and $^{20}Ne + ^{150}Nd$ to bring the $9n$ excitation functions into line with those for the $8n$ and $10n$ channels.[29]

III. RESULTS

The neutron spectra in the laboratory system from the four angles of 20°, 70°, 100°, and 151° relative to the beam direction are shown by the points in Figs. 1 and 2. The neutron spectra observed in coincidence with γ rays characteristic of $^{162,161,160}Yb$ nuclei are associated with $8n$, $9n$, and $10n$ emission and are shown in Figs. 1(a), 1(b), and 1(c), respectively. The neutron spectra associated with the production of ^{159}Er and ^{158}Er, the $\alpha 7n$ and $\alpha 8n$ products, are shown in Figs.

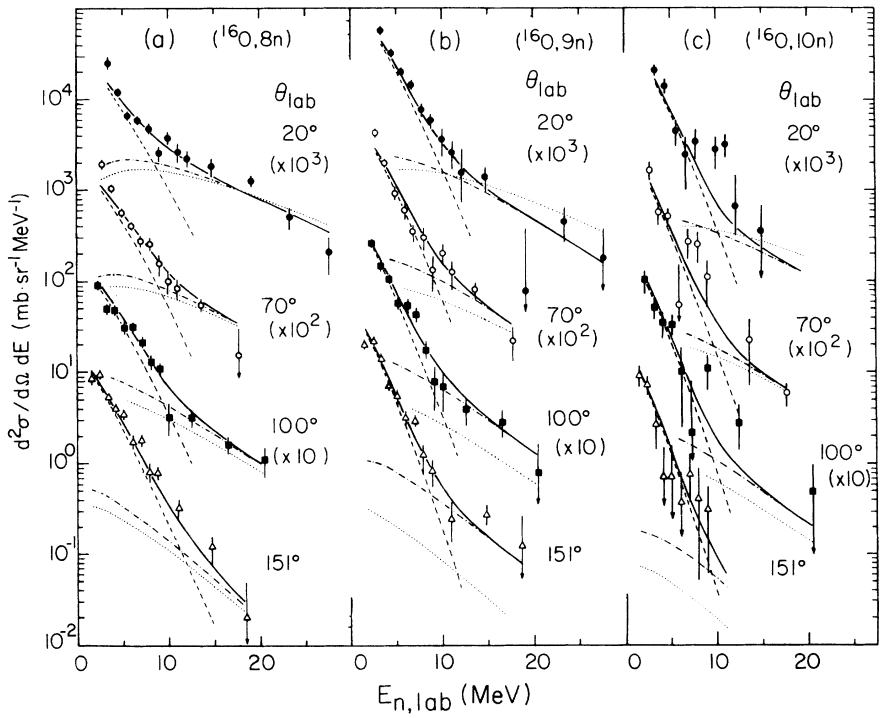

FIG. 1. Energy spectra of neutrons from 152 MeV ^{16}O on ^{154}Sm recorded by time of flight in coincidence with several transitions observed in the Ge(Li) detector characteristic of the $8n$, $9n$, and $10n$ exit channels. The points give the measured laboratory cross sections. The solid curves are the simultaneous least-squares fits to all the data of the spectrum from two independent moving sources. The dashed and dash-dotted curves give the spectra from the slower source (having the center-of-mass velocity) and the faster source, respectively. The dotted lines are the least-squares fits of the rapidly moving source with the velocity fixed by a classical orbiting model (see text).

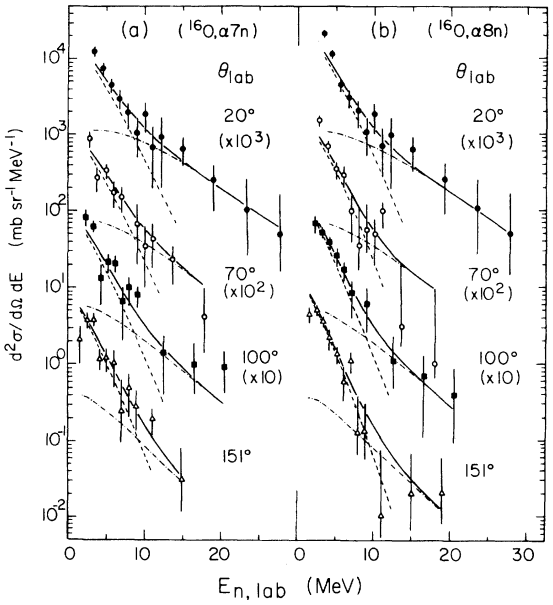

FIG. 2. Energy spectra of neutrons from 152 MeV ^{16}O on ^{154}Sm recorded by time of flight in coincidence with several transitions observed in the Ge(Li) detector characteristic of the $\alpha 7n$ and $\alpha 8n$ channels. The points give the measured laboratory cross sections. The curves have the same meaning as in Fig. 1.

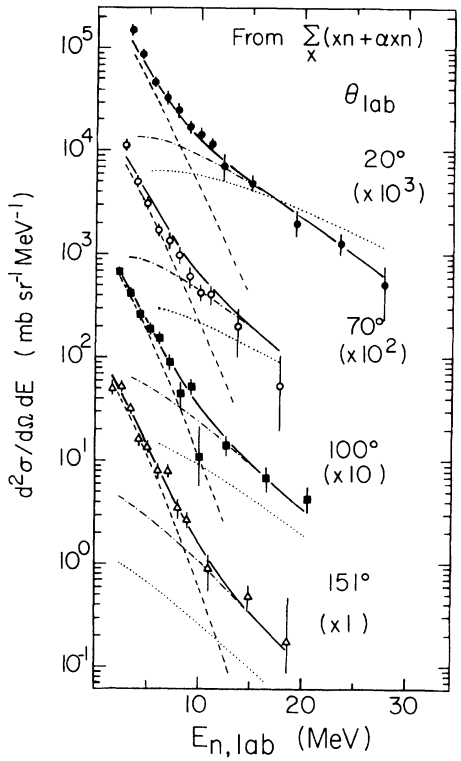

FIG. 3. Neutron energy spectra obtained from the sum of the five identified exit channels shown in Figs. 1 and 2. The curves have the same meaning as in Fig.1 and were obtained by an independent fit.

2(a) and 2(b). The enhanced emission of energetic neutrons at forward angle is clearly seen for the $8n$, $9n$, $\alpha 7n$, and $\alpha 8n$ products. The cross sections given in Figs. 1 and 2 when integrated over neutron energy and angle are in good agreement with the total cross sections for the corresponding exit channels given in the preceding paper.

In Fig. 3 we show the laboratory neutron spectra summed over the observed five exit channels from Figs. 1 and 2. These spectra represent the bulk of the neutron cross section for fusionlike processes, as the yields associated with other fusionlike products were much smaller.

The summed spectra of Fig. 3 and those from the (^{16}O, $8n$) channel are shown in Figs. 4(a) and 4(b), respectively, as a function of the center-of-mass angle (binary ^{169}Yb+n division) for various indicated c.m. neutron energies. The points are from the fits shown as solid lines in Figs. 3 and 1(a), respectively, and the lines are drawn to guide the eye. The correlations for the low neutron energies exhibit symmetry about 90° and a minimum at $\theta_{c.m.} = 90°$, as expected for equilibrated compound nucleus systems. For higher neutron energies progressively stronger forward peaking is observed in this frame of reference, indicating the presence of a non-compound mechanism.

The results shown in Figs. 1–3 are subject to the limited statistical accuracy introduced by the requirement for coincidences with peaks in the Ge(Li) detector. In order to present neutron spectra of better statistical accuracy, although from less well specified processes, we show in Fig. 5 neutron spectra coincident with any pulse observed in the Ge(Li) counter. This coincidence requirement introduces weights for the various exit channels comprising these spectra in accordance with their γ-ray multiplicity. Processes such as quasielastic or deep inelastic scattering that are probably associated with lower $\langle M_\gamma \rangle$ contribute less to the spectra of Fig. 5 than they would to singles measurements. The results in Fig. 5 are given in the center-of-mass system for a (^{169}Yb+n) binary division.

IV. ANALYSIS AND DISCUSSION

A. Comparison with the model for incomplete fusion

According to the incomplete fusion picture of Siwek-Wilzcynska *et al.*,[10] if the entrance channel angular momentum exceeds a critical angular momentum l_c, no fusion can occur unless the

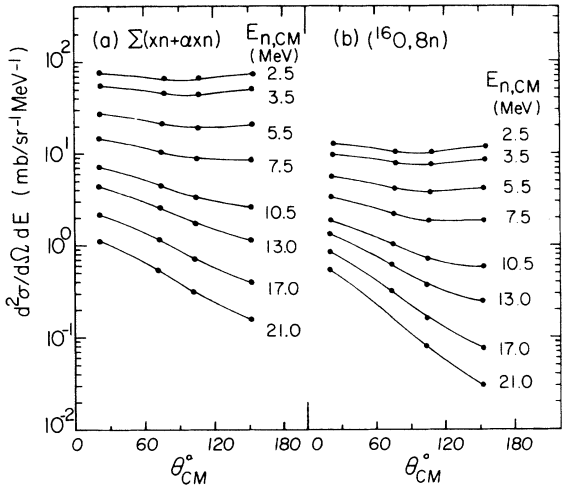

FIG. 4. Angular correlations of neutrons of the indicated energies associated with the sum of the observed fusion channels and with the (^{16}O, 8n) channel. The points are from two-component fits of the spectra.

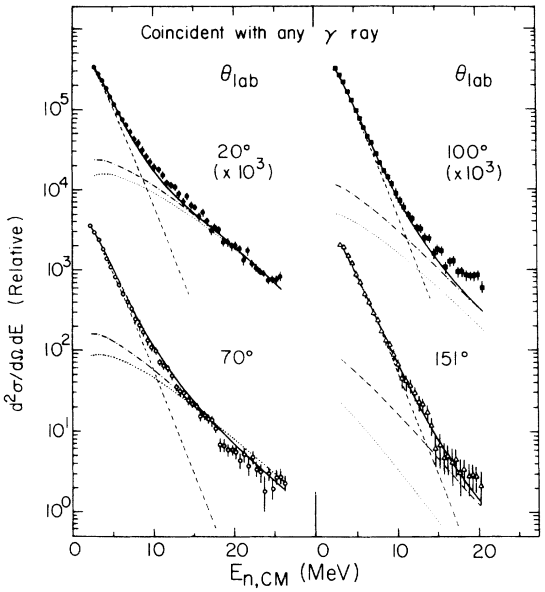

FIG. 5. Center-of-mass neutron spectra recorded by time of flight in coincidence with any pulse in the Ge(Li) detector. In addition to fusionlike events neutrons from other processes such as deep inelastic reactions contribute with weights in proportion to their γ-ray multiplicity. The curves have the same meaning as in Fig. 1.

projectile emits a fragment which removes enough angular momentum so that the orbital angular momentum of the remaining portion of the projectile is now below its own l_c for fusion with the target. This picture leads to a hierarchy of incomplete fusion processes in which successively larger pieces of the projectile are ejected. They are localized in l space at successively higher angular momenta, as has been observed experimentally for charged-particle fragments.[12,13] If we consider only (HI, xn) reactions, this hierarchy will correspond to emission of 1n, 2n, 3n, etc., from the projectile prior to fusion. The regions of the entrance channel l space in which these fast neutron emission processes are localized will overlap with regions in which other incomplete fusion processes can occur. For the ^{16}O + ^{154}Sm system the most important other exit channel will involve α emission from the projectile.[12] Since neutron emission from projectiles such as ^{12}C, ^{16}O, or ^{20}Ne cannot compete favorably with α emission for the same region of high l values because of the much higher neutron separation energy, significant fast neutron emission from incomplete fusion may not appear until the threshold energy for any incomplete fusion corresponding to l_c is appreciably exceeded in the entrance channel. This behavior was observed in the "threshold" for fast neutron emission discussed in Ref. 26 on the basis of saturation seen in the $\langle M_\gamma \rangle$ values as a function of beam energy.

The physical picture for incomplete fusion discussed in Ref. 10 involves the emission of fragments of the projectile very early in the reaction process when the projectile velocity may still be appreciably greater than the velocity $v_{c.m.}$ of the center of mass of the initial system. It seems therefore natural to describe the spectral shape of the fast neutrons in terms of emission from a fast moving source. For simplicity we adopt for the spectral shape in the rest frame of the source the form commonly used in studies of projectile fragmentation reactions[32-34] in high energy heavy-ion induced reactions, namely an isotropic Gaussian momentum distribution,

$$\frac{d^3\sigma}{dp^3} \propto \exp(-p^2/2s^2), \tag{1}$$

where p is the neutron momentum. The variance s^2 of the momentum distribution of fragments of mass number A_f from a source of mass number A_s in the rest frame of the source is related to the Fermi momentum p_F of the nucleons in the source by $s_0^2 = s^2(A_s - 1)/(A_s A_f - A_f^2) = p_F^2/5$. Goldhaber has shown[35] that an identical form for the fragment momentum distribution is obtained under the assumption that the excited projectile decays after attaining approximate thermal equilibrium. The width parameter for the neutron emission is then expressed in terms of the source temperature τ by

$$s_0^2 = M_n \tau (A_s - 1)/A_s, \tag{2}$$

where M_n is the nucleon mass.

Since the fast neutron spectra experimentally observed are superimposed on a spectrum due to evaporation of neutrons by the equilibrated fused system, we describe the observed neutron spectrum in the laboratory by a sum of two terms,

$$\frac{d^2\sigma}{dEd\Omega} = \frac{N_T E_n^{1/2}}{2(\pi T)^{3/2}} \exp\left[\frac{-(E_n - 2\sqrt{\gamma E_n}\cos\theta + \gamma)}{T}\right] + \frac{N_F{}^0 E_n^{1/2}}{2(\pi\tau)^{3/2}} \exp\left[\frac{-(E_n - 2\sqrt{\epsilon E_n}\cos\theta + \epsilon)}{\tau}\right]. \quad (3)$$

The first term in Eq. (3) gives the spectrum of the "soft" component, the neutrons evaporated by the fused system moving with the center-of-mass velocity $v_{c.m.}$. The constant N_T is proportional to the neutron multiplicity, T is the temperature, and $\gamma = \frac{1}{2} M_n v_{c.m.}{}^2$. For this equilibrium spectrum we have used the form derived by LeCouteur[36] for an equation of state $E^* = aT^2$, where E^* is the excitation energy and a is a constant, and we have approximated the $\frac{5}{11}$ exponent of E_n by $\frac{1}{2}$ in the pre-exponential factor. The second term in Eq. (3) represents the momentum distribution of Eq. (1) transformed to an energy and angular distribution with the momentum width s expressed in terms of the equivalent "temperature" τ from Eq. (2). The constant $N_F{}^0$ is proportional to the multiplicity of neutrons emitted by the fast moving source and $\epsilon = \frac{1}{2} M_n v_s{}^2$, where v_s is the velocity of the fast source. The emission of the neutrons from this source was assumed to be isotropic in its rest frame. The soft component was allowed to have an angular distribution given by

$$N_T = N_T{}^0[1 + A_2 P_2(\cos\theta_{c.m.})]$$

in its rest frame. The data support a small A_2 for the slow component, but the fast component appears to be consistent with isotropic emission in the frame of the fast moving source.

In fitting Eq. (3) to the data, the quantities $N_T{}^0$, $N_F{}^0$, A_2, ϵ, T and τ were allowed to vary. The effective temperature T for the soft component in this reaction is expected to be in the range of 1.4–2.0 MeV. The parameters deduced from these fits are summarized in Table I. The fraction f of fast neutrons is given by $f = N_T{}^0/(N_F{}^0 + N_T{}^0)$. The small number of fast neutrons associated with the $10n$ channel did not permit simultaneous variation of all the parameters; for this channel, and for $\alpha 8n$ as well, some parameters were held fixed. Parameters are also given from fits to the sum over the xn channels, over all the $(xn + \alpha xn)$ channels, and for neutrons in coincidence with any γ ray. The last column in Table I gives the velocity of the fast source in terms of v_p, which is the projectile velocity in the interaction region which corresponds to the projectile energy in excess of the Coulomb barrier (calculated with a radius parameter of 1.44 fm).

The solid lines in Figs. 1 and 2 are the fits to

TABLE I. Parameters from two-source fits to Eq. (3) of the neutron spectra from $^{16}O + ^{154}Sm$ at 152 MeV and $^{12}C + ^{158}Gd$ at 152 MeV (Ref. 7). The quantity $f = N_F{}^0/(N_F{}^0 + N_T{}^0)$ is the fraction of neutrons due to the fast component. A_2 is the coefficient of $P_2(\cos\theta)$ in the angular correlation of the soft component. The velocity of the moving source of fast neutrons, v_s, is expressed in terms of v_p, the projectile velocity above the Coulomb barrier. Underlined numbers are estimated statistical uncertainties in the least significant digits.

Reaction	$N_T{}^0$	$N_F{}^0$	A_2	f (%)	T (MeV)	τ (MeV)	v_s/v_p
$^{16}O + ^{154}Sm$							
$8n$	684 42	180 36	0.13 5	20.8 42	1.98 14	6.1 8	0.60 10
$9n$	2045 135	250 80	0.13[a]	10.9 36	1.55 10	5.4 11	0.36 15
$10n$	820 110	42 8	0.13[a]	4.9 11	1.41 14	5.77[a]	0.40[a]
$\alpha 7n$	380 47	91 32	0.10[a]	18.9 80	1.78 20	4.9 10	0.40 20
$\alpha 8n$	573 49	85 17	0.10[a]	12.9 29	1.62 15	4.9 15	0.40[a]
Σxn	3528 213	626 112	0.20[a]	15.0 29	1.51 8	5.2 6	0.40 15
$\Sigma(xn + \alpha xn)$	4429 215	890 220	0.20[a]	16.7 40	1.53 10	4.9 8	0.39 10
any γ	231 4	1.69 15	0.10[a]	6.8 6	1.59 2	4.27 12	0.28 2
$^{12}C + ^{158}Gd$							
$8n$	24 3	16.0 14	0[a]	40 6	1.7[a]	6.8 9	0.3 2
$9n$	43 3	15.3 14	0[a]	26 3	1.7[a]	8.1 12	0.25 26
$10n$	71 4	11.1 21	0[a]	13 3	1.7[a]	7.5 24	0.23 50

[a] Parameter kept constant for this fit.

Eq. (3) with the parameters given in Table I. The dashed and dash-dotted lines in Figs. 1 and 2 correspond, respectively, to the neutrons from the slow and fast moving sources. Similar results for the summed spectra of Fig. 3 are shown by the solid, dashed, and dash-dotted curves corresponding to the total, slow, and fast components of the neutron spectrum. From a comparison of the experimental data with these fits it is clear that Eq. (3) accounts very well for both the energy and angular correlations of the neutron spectra.

The most striking result from Table I is the velocity of the fast source, namely $v_s = (0.4 \pm 0.1)\, v_p$. A value considerably nearer v_p might be expected on the basis of the simple picture for incomplete fusion.[10] Indeed, the measured spectra of the energetic forward α particles,[6,8,10] carbon ions,[12] and hydrogen isotopes[11] tend to peak closer to the beam velocity. Although the charged particles are accelerated by the Coulomb repulsion in the exit channel while neutrons are not, this effect is much too small to account for the observed reduction of v_s. Taken literally, the present analysis leads one to conclude that fast neutron emission from the projectilelike particle requires that ~84% (i.e., 64 MeV) of the initial kinetic energy above the barrier is dissipated, presumably into excitation energy of the projectile and target system.

The interpretation of the momentum distribution width parameter s (or the equivalent τ) presents some difficulty. Spectra of fragments produced in relativistic heavy ion collisions have been analyzed[32] using the same formalism described here. It has been assumed that in such experiments fragments are produced by a sudden shearing of the projectile without prior excitation, so that the values of the width parameters obtained in the analysis should reflect the Fermi momentum of nucleons in the projectile.[37] A value of $s_0 = 86$ MeV/c has been obtained for fragmentation of 2.1 GeV/nucleon ^{16}O on a number of targets. This corresponds to a Fermi momentum $p_F = 192$ MeV/c, close to the value of ~230 MeV/c from measurements of electron scattering by ^{12}C and ^{24}Mg.[38] Recently, Scott has presented a similar analysis of ^{16}O-induced reactions over a wide range of energies.[37] For ^{16}O energies greater than 20 MeV/nucleon above the Coulomb barrier a constant $s_0 \sim 86$ MeV/c was obtained, but at lower energies s_0 was found to drop rapidly. Scott has conjectured that below 20 MeV/ nucleon there is sufficient time for some equilibration to take place so that the temperature parameter τ is relevant. The values of τ as a function of energy were shown[37] to be represented adequately by an equation of state of the form $E^* = aT^2 \propto (E_{c.m.} - V_c)$ with $a \approx (A/8)$ MeV^{-1}.

The width parameters obtained in our analysis, $s_0 = 73 \pm 5$ and 65 ± 5 MeV/c, are somewhat less than the "fragmentation limit" value of 86 MeV/c. The corresponding values of τ describing the fast component of the n spectrum are ~6 MeV for the xn channels and 4.9 ± 0.7 MeV for the sum over all xn and αxn channels. If the rather extreme picture of decaying of a hot equilibrated projectilelike object is adopted, the corresponding excitation energy of the source would be in the range $E^* = 35$–72 MeV. This would imply that at the time of neutron emission more than half the energy available from the deceleration is tied up in excitation of the projectile. Taken literally this would suggest that the neutrons are emitted very early in the reaction, before equilibration of energy in the projectile-target system has progressed very far. Stokstad[39] has estimated the mean time required for the emission of particles (nucleons or α-particles) to be $\tau_{part} \sim 0.5 \exp(13/T) \times 10^{-22}$ s, where T is the temperature

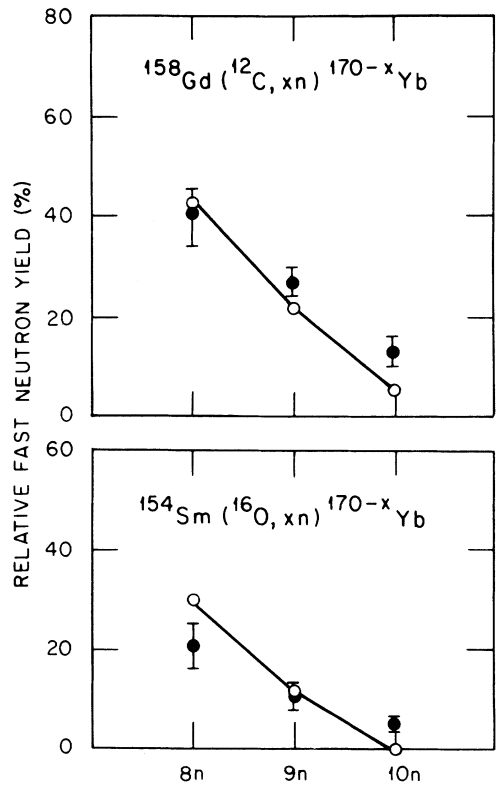

FIG. 6. Percent of fast neutrons from 152 MeV ^{16}O on ^{154}Sm for the xn channels. The full points are data obtained from the two-source fits shown in Fig. 1. The lines and the open points are predictions from Ref. 26 based on the incomplete fusion model.

of the source in MeV. Using this relation and the range of temperatures deduced from the fits to the neutron spectra we obtain an emission time of $4-7\times10^{-22}$ s. This is comparable to the $5-10\times10^{-22}$ s required for equilibration of the energy degree of freedom reported for deep inelastic collisions of ^{56}Fe on ^{165}Ho in Ref. 23. If this equilibration time is somewhat longer for the more asymmetric ^{16}O + ^{154}Sm system, the picture of decay of a hot, locally equilibrated projectile-like object, in a reaction destined to lead eventually to fusion-like final channels, might indeed have some validity. This of course supposes that on the microscopic level some sense can be made of a process which concentrates an appreciable fraction of the incident kinetic energy in the form of excitation of a projectilelike fragment.

The fit of the experimental spectra to Eq. (3) also provides the relative yields of the fast and slow components of the neutron spectrum. The full data points in Fig. 6 show the fraction f(%) for the fast component from Table I plotted against the number of emitted neutrons x identifying the exit channel. The open points connected by lines are the predictions of the incomplete fusion model as developed in the preceding paper. Remarkable agreement is seen for both the ^{16}O + ^{154}Sm system (present experiment) and the ^{12}C + ^{158}Gd data of Westerberg *et al.*[7] The latter spectra were fitted to Eq. (3) with the results shown in Table I. Since those spectra were measured at only two angles the velocity v_s of the fast source could not be defined as accurately, but the results are consistent with v_s/v_p for the ^{16}O + ^{154}Sm system within one standard deviation. For the C + Gd data, a fixed T = 1.7 MeV was used for all three xn channels. Trials with more realistic values of T, similar to those found for O + Sm, showed no significant changes in the results for f.

The fit to the neutron spectra obtained in the ^{16}O + ^{154}Sm reaction in coincidence with any γ ray (Fig. 5) has different characteristics from those corresponding to specific exit channels. The source velocity is smaller ($v_s/v_p = 0.28 \pm 0.2$) and the source has a lower temperature ($\tau = 4.27 \pm 0.12$ MeV). These results indicate that neutrons evaporated by accelerated fragments from quasi-elastic and deep inelastic processes show a weaker fast component than do the fusionlike processes.

B. Comparison with a classical orbiting model

An extension of the two component model was undertaken in order to investigate the origin of the reduced velocity of the fast moving source and the time scale of the reaction. Our data on γ-ray multiplicity suggest[26] that the fast neutron component is produced only for entrance channel angular momenta near the maximum for complete fusion l_c. We therefore adopt a classical description of the projectile motion with a single impact parameter corresponding to l_c. The projectile is assumed to approach the target along a Coulomb trajectory corresponding to l_c until a separation of $R = r_0(A_P^{1/3} + A_T^{1/2})$ is reached. At this point, following the simple picture of Bon-

TABLE II. Parameters from the classical orbiting model fit to the neutron spectra from ^{16}O + ^{154}Sm at 152 MeV (present data) and ^{12}C + ^{158}Gd at 152 MeV (Ref. 7). The parameters are as in Table I. The angle of rotation θ_{rot} is discussed in the text. Underlined numbers are estimated statistical uncertainties in the least significant digits.

Reaction	N_T^0	N_F^0	A_2[a]	f(%)	T (MeV)	τ (MeV)	θ_{rot}[a]
^{16}O + ^{154}Sm							
$8n$	740 50	150 20	0.20	16.9 25	1.99 11	6.8 9	40°
$9n$	2006 115	138 33	0.15	6.4 16	1.70 8	6.3[a]	40°
$10n$	800 100	32.6 62	0.20	3.9 7	1.46 14	6.3[a]	40°
Σxn	3542 189	312 55	0	8.1 15	1.72 8	7.7 19	40°
$\alpha 7n$	411 38	45 15	0	9.9 33	2.00 16	5.4 17	40°
$\alpha 8n$	620 50	27 6	0.15	4.2 9	1.74 11	6.3[a]	40°
$\Sigma(xn + \alpha xn)$	4576 244	413 80	0.20	8.2 17	1.74 7	5.8 10	40°
any γ	225 6	933 71	0	4.0 3	1.66 2	3.87 15	20°
^{12}C + ^{158}Gd							
$8n$	24 2	14 1	0	37 5	1.7[a]	5.6 6	20°
$9n$	44 2	13 1	0	23 2	1.7[a]	7.0 11	20°
$10n$	72 3	9.2 12	0	11 2	1.7[a]	4.8 15	20°

[a] Parameter kept constant for this fit.

dorf[40] or Gelbke *et al.*,[33] we assume that the radial motion suddenly stops and the radial kinetic energy is transferred into excitation energy of the fragments. Since l_c is the partial wave at which fusion just fails to occur, so that the attractive and repulsive forces are approximately equal, the reaction will proceed with the radial separation remaining nearly constant ("orbiting"), while the projectile moves with the angular velocity required to conserve angular momentum. If the neutron is assumed to be emitted during this period of orbiting, the source velocity and direction are fixed at any instant. Thus no free parameter for the source velocity is required in this description.

We find that the experimental data for the fast neutrons are reproduced reasonably well for emission occurring after rotations of $40° \pm 20°$ for the $^{16}O + ^{154}Sm$ data from identified fusion channels and $20° \pm 10°$ for the spectra gated by any γ. For the $^{12}C + ^{158}Gd$ data of Ref. 7, an angle of $20° \pm 10°$ gave reasonable results. The experimental spectra were fit by varying the parameters N_T^0, N_F^0, T, and τ, using the predicted velocity for the source having undergone a 40° or 20° rotation. The distance of closest approach was calculated with a radius parameter $r_0 = 1.1$ fm. The resulting parameters are summarized in Table II and the fits for the fast component are shown as the dotted curves in Figs. 1(a)–1(c), 2(a), and 2(b). Reasonable agreement with experiment is obtained for all exit channels. In particular the fit to the $8n$ channel, where the fast neutrons are most intense, is remarkably good (compare also Table I and II).

It is interesting to consider the rotation times in this picture. We find that for ^{16}O on ^{154}Sm, $d\theta/dt \simeq 2.4 \times 10^{22}$ rad/s, so 40° takes 2.9×10^{-22} s. Usually one allows for loss of relative angular momentum (and hence of angular velocity) into intrinsic motion via tangential friction. In the rolling limit the angular momentum (and angular velocity) is reduced by a factor of $\frac{5}{7}$. In this case the fits to the data improve somewhat and the 40° rotation time is increased to 4.1×10^{-22} s. It is interesting at this point to recall that the mean time for particle emission from an object with a temperature of 6 MeV is $\sim 4 \times 10^{-22}$ s, according to the relation given by Stokstad.[39]

C. Comparison with the PEP model

We have compared the present results for the $^{16}O + ^{154}Sm$ system at 152 MeV with detailed calculations[41] using the model of prompt emission of particles of Bondorf *et al.*[18,19] The calculations were made for the approximate center-of-mass angle corresponding approximately to the average

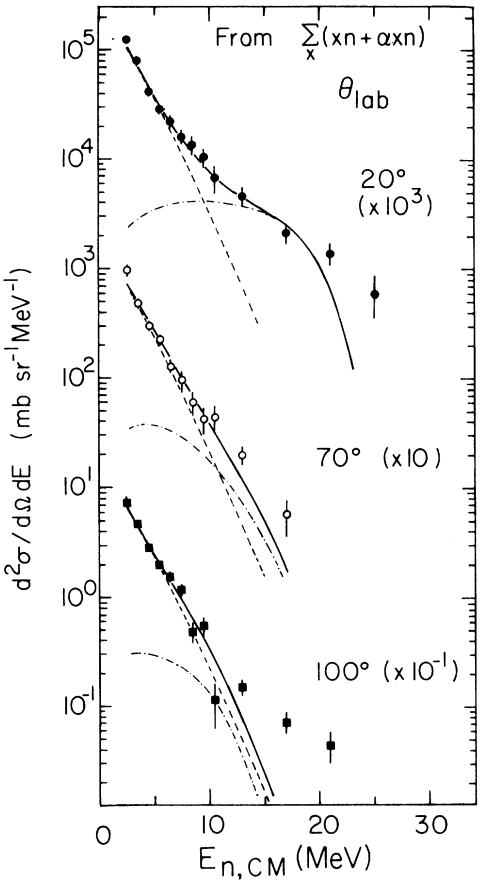

FIG. 7. Comparison of the summed neutron spectra from Fig. 3 (points) with the predictions (Ref. 41) of the PEP model of Ref. 19 (dashed-dotted curves). The dashed lines are the fits for the equilibrium neutrons with temperature fixed at 1.8 MeV. The full curves are the theoretical curves [Eq. (4)] that give the best least-squares fits to the experimental data.

neutron energy of each spectrum. Collisions with l up to 68.6 were included. The calculations do not distinguish between individual exit channels and so have been compared with the sum over the xn and αxn channels. Since considerable equilibrium emission of neutrons is present in the data, we have fitted the summed spectra from the xn and αxn channels using the expression

$$y(E_n) = A E_n^{1/2} e^{-E_n/T} + B P_{\mathrm{PEP}}(E_n), \tag{4}$$

where E_n is the neutron energy in the center-of-mass system ($^{169}Yb + n$ binary division), $P_{\mathrm{PEP}}(E_n)$ is the theoretical spectrum, and A and B are normalization constants. A fit with $B = 1$ would imply that the model successfully predicts the magnitude of the fast component. The fits for $\theta_{lab} = 20°$, 70°, and 100° are shown in Fig. 7, obtained with an equilibrium component of temperature 1.8 MeV. The theoretical spectra un-

derestimate the emission of high energy neutrons, and the disagreement with experiment increases with laboratory angle. However, least-squares values of B [Eq. (4)] for the three angles fitted were found to be 0.96 ± 0.19, 1.4 ± 0.7, and 1.1 ± 1.0, encouragingly near the expected value of unity. The large uncertainty in B, increasing with angle, is due to the increasing similarity of the slopes of the PEP spectra at higher neutron energy with those of the equilibrium component; at 151° the PEP normalization could not be determined at all. From these values of B it can be said that the 20° cross section is reasonably well reproduced but meaningful conclusions for larger angles are not possible.

D. Comparison with a hot spot model

Garpman *et al.*[42] have calculated relative cross sections for neutron emission from a hot spot of uniform temperature. The refraction effect due to the boundary was taken into account, but cooling due to sharing of energy with the nucleons outside the spot was not considered, and the calculations were restricted to collisions with zero impact parameter. Reference 42 compares results for a hot spot of normal nuclear density and a radius 70% of that for the amalgamated system with preliminary data from the present experiment. The calculations represent the angular and energy dependence of the data fairly well although they tend to overestimate the yield of the highest-energy neutrons at back angles. It is interesting that this model does well in spite of its restriction to $l = 0$ collisions. More recently this model has been extended to allow for a nonzero impact parameter[43] and convective cooling,[44] and it has been combined with the PEP model.[44]

V. CONCLUSIONS

From our analysis of neutron spectra from $^{16}O + ^{154}Sm$ and $^{12}C + ^{158}Gd$ we find that the yield of fast neutrons as a function of x in (HI, xn) fusionlike reactions agrees well with the predictions[26] of the incomplete fusion model with successive critical angular momenta.[10] The energy spectra and angular correlations can be explained by the assumption that the fast neutrons are emitted from a rapidly moving source. In a fusion reaction this source can only be associated with the projectile motion. We find that the source velocity required to fit the data is appreciably less than the projectile velocity, but similar to the velocity for the projectile orbiting the target with angular momentum l_c. These findings and those of the preceding paper[26] are consistent with the interpretation that incomplete fusion is responsible for the emission of fast neutrons in the observed fusion-like channels. Of course, this consistency should not be interpreted to exclude contributions from other mechanisms or to deduce that other pictures might not account for all the data equally well. The incomplete fusion picture is not a microscopic theory and does not attempt to describe the processes responsible for the emission of particles prior to fusion. This has allowed us to extend the concept of incomplete fusion to include emission from an appreciably damped projectile. A more detailed treatment of the pre-fusion excitation and emission process, with full attention to the l distributions, is needed even if the interpretation of the data presented here proves to be basically correct.

ACKNOWLEDGMENTS

Oak Ridge National Laboratory is operated by Union Carbide Corporation for the U. S. Department of Energy under Contract No. W-7405-eng-26. This work was supported by the DOE Division of Basic Nuclear Sciences, in part under Contract No. DE-A502-76ER-4052, and by travel grants from Oak Ridge Associated Universities.

---

*Present address: Fusion Energy Division, Oak Ridge National Laboratory, Oak Ridge, Tennessee 37830.
†Present address: DPh-N/BE, CEN Saclay, 91191 Gif-sur-Yvette Cedex, France.
‡Present address: South Carolina Electric & Gas Co., Columbia, South Carolina 29218.

[1]M. Blann, Annu. Rev. Nucl. Sci. 25, 123 (1975); Phys. Rev. C 23, 205 (1981).
[2]H. C. Britt and A. R. Quinton, Phys. Rev. 124, 877 (1961).
[3]J. Galin, B. Gatty, D. Guerreau, C. Rousset, U. C. Schlotthauer-Voos, and X. Tarrago, Phys. Rev. C 9, 1126 (1974).
[4]E. J. Hoffman and D. G. Sarantites, Nucl. Phys. A173, 177 (1971); J. H. Barker and D. G. Sarantites, Phys. Rev. C 9, 607 (1974).
[5]M. L. Halbert, P. O. Tjøm, I. Espe, G. B. Hagemann, B. Herskind, M. Neiman, and H. Oeschler, Nucl. Phys. A259, 496 (1976).
[6]T. Inamura, M. Ishihara, T. Fukuda, T. Shimoda, and H. Hiruta, Phys. Lett. 68B, 51 (1977).
[7]L. Westerberg, D. G. Sarantites, D. C. Hensley, R. A. Dayras, and J. H. Barker, Phys. Rev. C 18, 796 (1978).
[8]D. R. Zolnowski, H. Yamada, S. E. Cala, A. C. Kahler, and T. T. Sugihara, Phys. Rev. Lett. 41, 92 (1978).
[9]K. A. Geoffroy, D. G. Sarantites, L. Westerberg, D. C. Hensley, R. A. Dayras, and M. L. Halbert, Bull. Am. Phys. Soc. 23, 950 (1978).
[10]K. Siwek-Wilczynska, E. H. du Marchie van Voorthuysen, J. van Popta, R. H. Siemssen, and J. Wilczynski, Phys. Rev. Lett. 42, 1599 (1979); Nucl. Phys. A330,

150 (1979).
[11]H. Yamada, D. R. Zolnowski, S. E. Cala, A. C. Kahler, J. Pierce, and T. T. Sugihara, Phys. Rev. Lett. 43, 605 (1979).
[12]K. A. Geoffroy, D. G. Sarantites, M. L. Halbert, D. C. Hensley, R. A. Dayras, and J. H. Barker, Phys. Rev. Lett. 43, 1303 (1979).
[13]J. H. Barker, J. R. Beene, M. L. Halbert, D. C. Hensley, M. Jääskeläinen, D. G. Sarantites, and R. Woodward, Phys. Rev. Lett. 45, 424 (1980).
[14]T. Kishimoto and K.-I. Kubo, Progress in Research, 1978–1979, Cyclotron Institute, Texas A & M University (unpublished).
[15]T. Udagawa and T. Tamura, Phys. Rev. Lett. 45, 1311 (1980).
[16]P.-A. Gottschalk and M. Weström, Phys. Rev. Lett. 39, 1250 (1977).
[17]M. C. Robel, Ph.D. thesis, Lawrence Berkeley Laboratory, 1979 (unpublished).
[18]J. P. Bondorf, J. N. De, A. O. T. Karvinen, G. Fái, and B. Jakobsson, Phys. Lett. 84B, 163 (1979).
[19]J. P. Bondorf, J. N. De, G. Fái, A. O. T. Karvinen, B. Jakobsson, and J. Randrup, Nucl. Phys. A333, 285 (1980).
[20]H. Ho, P. L. Gonthier, M. N. Namboodiri, J. B. Natowitz, L. Adler, O. Martin, P. Kasiraj, A. Khodai, S. Simon, and K. Hagel, Bull. Am. Phys. Soc. 24, 833 (1979).
[21]G. A. Petitt, R. L. Ferguson, A. Gavron, F. E. Obenshain, F. Plasil, A. H. Snell, G. R. Young, K. A. Goeffroy, D. G. Sarantites, and C. F. Maguire, Proceedings of the International Symposium on Continuum Spectra of Heavy Ion Reactions, San Antonio, Texas, 1979 (Harwood, New York, 1980), p. 319; A. Gavron, R. L. Ferguson, F. E. Obenshain, F. Plasil, G. R. Young, G. A. Petitt, K. Geoffroy Young, D. G. Sarantites, and C. F. Maguire, Phys. Rev. Lett. 46, 8 (1981).
[22]H. Gemmeke, P. Netter, Ax. Richter, L. Lassen, S. Lewandowski, W. Lücking, and R. Schreck, Phys. Lett. 97B, 213 (1980).
[23]D. Hilscher, J. R. Birkelund, A. D. Hoover, W. U. Schröder, W. W. Wilcke, J. R. Huizenga, A. C. Mignery, K. L. Wolf, H. F. Breuer, and V. E. Viola, Jr., Phys. Rev. C 20, 576 (1979).
[24]Y. Eyal, A. Gavron, I. Tserruya, Z. Fraenkel, Y. Eisen, S. Wald, R. Bass, G. R. Gould, G. Kreyling, R. Renfordt, K. Stelzer, R. Zitzmann, A. Gobbi, U. Lynen, H. Stelzer, I. Rode, and R. Bock, Phys. Rev. Lett. 41, 625 (1978).
[25]D. G. Sarantites, L. Westerberg, M. L. Halbert, R. A. Dayras, D. C. Hensley, and J. H. Barker, Phys. Rev. C 18, 774 (1978).
[26]J. R. Beene, M. L. Halbert, D. C. Hensley, R. A. Dayras, K. Geoffroy Young, D. G. Sarantites, and J. H. Barker, preceding paper, Phys. Rev. C 23, 2463 (1981).
[27]L. Westerberg, D. G. Sarantites, R. Lovett, J. T. Hood, J. H. Barker, C. M. Currie, and N. Mullani, Nucl. Instrum. Methods 145, 295 (1977).
[28]D. G. Sarantites, J. H. Barker, M. L. Halbert, D. C. Hensley, R. A. Dayras, E. Eichler, N. R. Johnson, and S. A. Gronemeyer, Phys. Rev. C 14, 2138 (1976).
[29]D. G. Sarantites, L. Westerberg, R. A. Dayras, M. L. Halbert, D. C. Hensley, and J. H. Barker, Phys. Rev. C 17, 601 (1978).
[30]J. E. Draper, Rev. Sci. Instrum. 37, 969 (1966).
[31]L. L. Riedinger, Nucl. Phys. A347, 141 (1980).
[32]D. E. Greiner, P. J. Lindstrom, H. H. Heckman, B. Cork, and F. S. Bieser, Phys. Rev. Lett. 35, 152 (1975).
[33]C. K. Gelbke, C. Olmer, M. Buenerd, D. L. Hendrie, J. Mahoney, M. C. Mermaz, and D. K. Scott, Phys. Rep. 42, 313 (1978).
[34]C. K. Gelbke, D. K. Scott, M. Bini, D. L. Hendrie, J. L. Laville, J. Mahoney, M. C. Mermaz, and C. Olmer, Phys. Lett. 70B, 415 (1977).
[35]A. S. Goldhaber, Phys. Lett. 53B, 306 (1974).
[36]K. J. LeCouteur, Proc. Phys. Soc. London A65, 718 (1952); K. J. LeCouteur and D. W. Lang, Nucl. Phys. 13, 32 (1959).
[37]D. K. Scott, International School of Physics "Ettore Majorana," Erice, Sicily, 1979, Lawrence Berkeley Laboratory Report No. LBL-8931, 1979 (unpublished).
[38]M. Moniz, I. Sick, R. R. Whitney, J. R. Ficenec, K. D. Kephart, and W. P. Trower, Phys. Rev. Lett. 26, 445 (1971).
[39]R. G. Stokstad, *Proceedings of the Topical Conference on Heavy-Ion Collisions, Fall Creek Falls State Park, Tennessee*, Report, No. CONF-770602 (U. S. Dept. of Commerce, Washington, D. C., 1977).
[40]J. P. Bondorf, *Nuclear Spectroscopy and Nuclear Reactions with Heavy Ions, Proceedings of the International School of Physics, "Enrico Fermi", Course LXII*, edited by H. Faraggi and R. A. Ricci (North-Holland, Amsterdam, 1976).
[41]J. P. Bondorf and A. Karvinen, private communication.
[42]S. I. A. Garpman, D. Sperber, and M. Zielinska-Pfabe, Phys. Lett. 90B, 53 (1980).
[43]W. W. Morrison, S. K. Samadarr, D. Sperber, and M. Zielinska-Pfabe, Phys. Lett. 93B, 379 (1980).
[44]P. Mooney, W. W. Morison, S. K. Samadarr, D. Sperber, and M. Zielinska-Pfabe, Phys. Lett. 98B, 240 (1981).